

Limnol. Oceanogr., 51(1, part 2), 2006, 488–503
© 2006, by the American Society of Limnology and Oceanography, Inc.

A comparative study of responses in planktonic food web structure and function in contrasting European coastal waters exposed to experimental nutrient addition

Y. Olsen

Department of Biology, Norwegian University of Science and Technology, N 7491 Trondheim, Norway

S. Agustí

Instituto Mediterráneo de Estudios Avanzados (IMEDEA), CSIC-UIB, Miquel Marqués 21, 07190, Mallorca, Spain

T. Andersen

Department of Biology, University of Oslo, P.O. Box 1066 Blindern, N-0316 Oslo, Norway

C. M. Duarte

Instituto Mediterráneo de Estudios Avanzados (IMEDEA), CSIC-UIB, Miquel Marqués 21, 07190, Mallorca, Spain

J. M. Gasol

Institut de Ciències del Mar, CMIMA-CSIC, Passeig Marítim de la Barceloneta, 37-49, E08003 Barcelona, Spain

I. Gismervik

Department of Biology, University of Oslo, P.O. Box 1066 Blindern, N-0316 Oslo, Norway

A.-S. Heiskanen

Plankton Ecology Group/Impacts Research Division, Finnish Environment Institute, P.O. Box 140, FIN-00251 Helsinki, Finland

E. Hoell

Hydro Research Center, Box 2560, 3901 Porsgrunn, Norway

*P. Kuuppo and R. Lignell*¹

Plankton Ecology Group/Impacts Research Division, Finnish Environment Institute, P.O. Box 140, FIN-00251 Helsinki, Finland

H. Reinertsen

Department of Biology, Norwegian University of Science and Technology, N 7491 Trondheim, Norway

*U. Sommer and H. Stibor*²

Institut für Meereskunde (IFM), Abteilung Meeresbotanik, Dusternbrooker Weg 20, DE-24105 Kiel, Germany

T. Tamminen

Plankton Ecology Group/Impacts Research Division, Finnish Environment Institute, P.O. Box 140, FIN-00251 Helsinki, Finland

¹ Present address: Finnish Institute of Marine Research, P.O. Box 33, FIN-00931 Helsinki, Finland.

² Present address: Department of Zoology, University of Munich, D-80333, Germany.

³ Present address: Department of Biotechnology, Norwegian University of Science and Technology, N 7491 Trondheim, Norway.

Acknowledgments

Thanks to our colleague Egil Sakshaug for his efforts with this manuscript. We also thank Stephen V. Smith and two anonymous reviewers for their constructive comments and help to improve our manuscript.

The work presented was undertaken jointly by the mesocosm partners of COMWEB, a project of the ELOISE Programme that was funded by the MAST Programme (MAST3-CT96-0052). The MED experiment received additional funding through a grant from the Spanish Commission for Science and Technology and the Research Council of Norway has contributed to the final scientific treatment of the NOR experiment. The comprehensive base of results derived is a result of the hard work of all the enthusiastic project participants and of all the partners involved in the experiments carried out in Tvärminne, Blanes, and Hopavågen.

*O. Vadstein*³

Department of Biology, Norwegian University of Science and Technology, N 7491 Trondheim, Norway

D. Vaqué

Institut de Ciències del Mar, CMIMA-CSIC, Passeig Marítim de la Barceloneta, 37-49, E08003 Barcelona, Spain

M. Vidal

Departament d'Ecologia, Universitat de Barcelona, Diagonal 645, E08028 Barcelona, Spain

Abstract

We quantify, compare, and generalize responses of experimental nutrient loadings (L_N) on planktonic community structure and function in coastal waters. Data were derived from three mesocosm experiments undertaken in Baltic (BAL), Mediterranean (MED), and Norwegian (NOR) coastal waters. A planktonic model with seven functional compartments and 30–32 different carbon flows fit to all three experiments was used as a framework for flow-rate estimation and comparison. Flows were estimated on the basis of time series of measured biomass, some measured flows, and inverse modeling. Biomass and gross uptake rate of carbon of most groups increased linearly with increasing L_N in the nutrient input range of 0–1 $\mu\text{mol N L}^{-1} \text{d}^{-1}$ at all locations. The fate of the gross primary production (GPP) was similar in all systems. Autotrophic biomass varied by two orders of magnitude among locations, with the lowest biomass and response to nutrient addition in MED waters. The variation of GPP among sites was less than one order of magnitude. Mesozooplankton dominated by doliolids (Tunicata), but not those dominated by copepods, presumably exerted efficient control of the autotrophic biomass, thereby buffering responses of autotrophs to high nutrient input. Among the many factors that can modify the responses of autotrophs to nutrients, the time scale over which the enrichment is made and the precise mode of nutrient enrichment are important. We suggest a general concept that may contribute to a scientific basis for understanding and managing coastal eutrophication.

Coastal eutrophication caused by human activities (anthropogenic eutrophication) is a problem in densely populated coastal regions throughout the world. Reports describing causes and consequences of enhanced anthropogenic nutrient emission to the coastal zone are numerous (e.g., Schiewer 1998; Colijn et al. 2002). Although it has been shown beyond reasonable doubt that increased nutrient inputs increase the primary production and phytoplankton biomass, there is also evidence for an order-of-magnitude difference in biomass yield per unit of nutrient input among systems (e.g., Nixon and Pilson 1983; Borum 1996; Cloern 2001). The ability to predict the ecological response of increased nutrient inputs, however, is still relatively poor. The ultimate challenge is to establish a simple and unified concept that can form a scientific basis for managing coastal waters. Freshwater management methods based on simple input–output models are not directly applicable to coastal waters (e.g., Vollenweider 1976), but can serve to inspire development of appropriate models.

Although autotrophic organisms respond to increased nutrient loading, the variability in the quantitative response (e.g., Cloern 2001) demonstrates that factors other than nutrient loading rate and nutrient concentration affect autotrophic biomass. The underlying reasons are probably complex, but there is a growing understanding that direct or indirect predation can affect the structure of the planktonic food web, thereby mitigating the growth and biomass response of autotrophs (Sommer and Stibor 2002; Stibor et al. 2004; Vadstein et al. 2004). These interactions have been studied more extensively in freshwater ecosystems, but there are uncertainties as to whether cascading effects from high trophic levels act on the autotrophs and the small heterotrophs in

marine systems (Shurin et al. 2002; Sommer and Stibor 2002). We know, however, that large grazers affect the lower food web structure through predation (Stibor et al. 2004; Vadstein et al. 2004). Predators therefore likely contribute to the buffering of the response of autotrophs that follows enhanced nutrient supply.

Our objective is to quantify, compare, and generalize short-term (<3 weeks) responses of planktonic food web structure and function of contrasting coastal plankton communities to different nutrient inputs. The experiments include all main plankton groups. Nitrogen (N) and phosphorus (P) were supplied in proportions close to the requirements of autotrophic organisms in natural marine systems. We particularly emphasize identification of major response similarities among three experimental sites. Moreover, we have sought to identify general patterns in the response of planktonic food webs of possible use for coastal management, thus contributing to a better understanding of how planktonic ecosystems respond.

Data for short-term responses of different nutrient inputs on autotrophic and heterotrophic functional plankton groups were obtained from three comprehensive, coordinated mesocosm experiments carried out in Baltic (BAL), Norwegian (NOR), and Mediterranean (MED) coastal waters. The experiments were carried out in relatively large mesocosms with equal design, with similar fertilization treatments, sampling, data processing, and scientific approach. The analytical methods were harmonized as far as possible. We used a gradient design instead of replicated treatments because the extended gradient design allows parameterization of the responses to different nutrient inputs. The goodness of fit of the data to the models can be assessed with regression anal-

Table 1. Review of experimental conditions of mesocosm experiments. Locations: BAL, Baltic Sea (southern Finland, Tvärminne); MED, Mediterranean Sea (northeastern Spain, Bay of Blanes); NOR, Norwegian Coastal current (northeastern Atlantic, central Norway).

Parameter	BAL	MED	NOR
Site description	>500 m from shore, depth >20 m	>700 m from shore, depth >35 m	>200 m from shore, depth >20 m
Experimental period	Jul–Aug 1996, 21 d	Jun–Jul 1997, 21 d	Aug–Sep 1997, 18 d
Mesocosm characteristics	8 units (conical), depth 14 m, diameter 2.3 m, volume 51 m ³	5 units (conical, not filled), depth 14 m, diameter 2 m, volume 35 m ³	7 units (conical), depth 12 m, diameter 2 m, volume 38 m ³
Sampling	Sampled every day, 11 main sampling days, integrated sample from 0–5 m and 6–12 m	Sampled every second day, 11 main sampling days, integrated sample (1–12 m)	Sampled every day, 11 main samplings (replicate at day 17), integrated sample (1–10 m)
Temperature (°C)	9–14	19–21	15–16
Salinity	6	38	31
Inorganic N doses ($\mu\text{mol L}^{-1} \text{ day}^{-1}$)	0, 0.14, 0.29, 0.44, 0.59, 0.74, 0.88, 1.03	0, 0.32, 0.64, 2.54, 5.09	0, 0.15, 0.26, 0.44, 0.75, 1.27, 2.16
Nutrient ratios (mol)	N:Si:P = 16:16:1	N:Si:P = 20:7:1	N:Si:P = 16:16:1

ysis. We used an established inverse method similar to that of Vézina and Platt (1988) to estimate the complete set of carbon flows in coastal planktonic food webs.

Earlier papers from these experiments have reported development of ciliates and mesozooplankton in NOR (Gismervik et al. 2002) and dissolved inorganic nutrient concentrations, phytoplankton biomass, and community structure in MED (Duarte et al. 2000).

Materials and methods

Experimental design and nutrient addition—Data were obtained from three jointly undertaken, coordinated mesocosm experiments of equal design, including a total of 20 mesocosms (depth 12–14 m, diameter 2.0–2.3 m, volume 30–50 m³) that were sampled 10–21 times during a period of 19–21 d (Table 1). The food web carbon flows were estimated using inverse mathematical methods (see following) based on time series for the measured biomasses, concentrations of dissolved and particulate carbon, and selected flow measurements. The three experimental coastal locations were very different (Table 1): (1) the Tvärminne archipelago in the Baltic Sea, southwestern coast of Finland (average summer chlorophyll *a* [Chl *a*] of 2–4 mg m⁻³; Lignell 1990); (2) a Mediterranean location off the coast of Blanes, northeastern Spain (average summer Chl *a* of 0.2 mg m⁻³; Duarte et al. 2000); and (3) a tide-driven Norwegian lagoon system at the coast of central Norway, Hopavågen (average summer Chl *a* of 1–3 mg m⁻³).

Water was enclosed by successive sinking to 10–14-m depth and lifting of the enclosures. The MED mesocosms were only two-thirds filled to prevent rupture from wave action due to the exposed location. If needed, volumes were adjusted by pumping and the mesocosms were moored to keep them apart, thus minimizing shading. The mesocosms were efficiently mixed by wave action propagating through the flexible walls.

Each experimental run involved 5–8 mesocosms that were run as single-factor experiments of 18–21-d duration, with different daily nutrient enrichment to the mesocosms at con-

stant N:Si:P ratio (Table 1). Nutrient addition, sampling, and operational procedures were similar, but adapted to the local conditions. A general objective was to ensure that the maximum enrichment resulted in saturation of the autotrophic biomass response. The highest maximum enrichment was therefore given to MED and the lowest to BAL (Table 1). The range was 0–1 $\mu\text{mol N L}^{-1} \text{ d}^{-1}$ for BAL (linear series of loadings, 50% NO_3^- and 50% NH_4^+); 0–5.1 $\mu\text{mol N L}^{-1} \text{ d}^{-1}$ for MED (exponential series of loadings, 100% NH_4^+); and 0–2.2 $\mu\text{mol N L}^{-1} \text{ d}^{-1}$ for NOR (exponential series of loadings, 50% NO_3^- and 50% NH_4^+). BAL and NOR were enriched with nutrients every day and MED every second day. The nutrients were delivered by lowering an open-ended plastic tube of 10–12-m length to about 1–2 m above the bottom of the mesocosms, followed by filling of the tube with nutrient solution with a volume equal to that of the tube, and finally emptying the tube by lifting it to the surface. No visible growth of attached organisms on mesocosm walls was observed during the experiments.

Sampling and analytical methods—Integrated water samples (0–6 m from BAL, 0–13 m from MED, 0–10 m from NOR) were collected and transferred to 25-liter containers at 0600–0830 h every day in BAL and NOR, and every second day in MED. From the pooled sample, phytoplankton and microzooplankton samples were taken every second day and preserved with 5 ml L⁻¹ acidic Lugol or glutaraldehyde (in MED, 1% final concentration). Bacteria including Archaea, picocyanobacteria, and heterotrophic nanoflagellates were preserved with glutaraldehyde (in MED, paraformaldehyde, 1% final concentration). Mesozooplankton were sampled every second to fourth day using a net (<100 μm) or integrated water samplers. If the latter, the plankton were subsequently collected into 25-liter containers and concentrated on a 35- μm screen. All of the mesozooplankton samples were preserved with 5 ml L⁻¹ acid Lugols. Each mesozooplankton sampling removed <0.1% of the standing stock in BAL and NOR and <2% in MED.

The food web (dominant taxonomic groups; Table 2) was divided into three size classes of autotrophs and four groups

Table 2. Review of dominant groups of organisms assigned to the functional food web components and references for principal methods for estimation of biomass. BB, biovolume-based estimate; LB, length-based estimate; MS, obtained with microscope; IA, obtained by image-analyzing system; FC, obtained by flow cytometer (Duarte et al. 2000).

Food web component	Location		
	BAL	MED	NOR
A1 pico-autotrophs	Picocyanobacteria, <2 μm , BB-MS, 0.22 pg C μm^{-3}	Picocyanobacteria, <2 μm , BB-FC, 0.123 pg C μm^{-3} (Waterbury et al. 1986)	Picocyanobacteria, <2 μm , BB-IA, 0.21 pg C μm^{-3} (Booth 1993)
A2 nano-autotrophs	Autotrophic and mixotrophic flagellates (2–10 μm), BB-MS, 0.11 pg C μm^{-3}	Autotrophic and mixotrophic flagellates (2–10 μm), autotrophic ciliates, BB-FC, 0.22 pg C μm^{-3} (Børnheim and Bratbak 1987)	Diatoms, <20 μm , auto-trophic flagellates, small dinoflagellates <20 μm , BB-MS, group-specific regressions (Strathmann 1967)
A3 micro-autotrophs	<i>Heterocapsa triquetra</i> , 15–25 μm , BB-MS, 0.11 pg C μm^{-3}	Diatoms and dinoflagellates, >10 μm , BB-MS, group-specific regressions (Strathmann 1967)	Diatom colonies, dino-flagellates, autotrophic ciliates, BB-MS, group-specific regressions (Strathmann 1967)
H1 pico-heterotrophs	Bacteria, <1 μm , BB-MS, 0.10 pg C μm^{-3} (Fagerbakke et al. 1996)	Bacteria, <1 μm , BB-FC, pg C cell ⁻¹ = 0.12 (μm^3 Cell ⁻¹) ^{0.7} (Norland 1993)	Bacteria, <1 μm , BB-IA, 0.16 pg C μm^{-3} (Vadstein and Olsen 1989)
H2 nano-heterotrophs	Flagellates (heterotrophic nanoflagellates, 2–10 μm), BB-MS, 0.22 pg C μm^{-3} (Børnheim and Bratbak 1987)	Flagellates (heterotrophic nanoflagellates, 2–10 μm), BB-FC, 0.22 pg C μm^{-3} (Børnheim and Bratbak 1987)	Flagellates (heterotrophic nanoflagellates, 2–8 μm), bacterivore ciliates, BB-IA, 0.22 pg C μm^{-3} (Børnheim and Bratbak 1987)
H3 micro-heterotrophs	Ciliates, >20 μm , rotifers, dinoflagellates, copepod nauplii, BB-MS, 0.20 pg C μm^{-3} (Putt and Stoecker 1989); copepods, see H4	Ciliates, >20 μm , BB-MS, 0.20 pg C μm^{-3} (Putt and Stoecker 1989); tintinnids, 0.053 pg C per μm^3 (lorica volume) ⁻¹ (Verity and Langdon 1984)	Ciliates, 20–50 μm , appendicularia, copepod nauplii, BB-MS, 0.19 pg C μm^{-3} (Putt and Stoecker 1989); for copepods, see H4
H4 meso-heterotrophs	Calanoid copepods, cladocerans, BB-MS, 0.052 pg C μm^{-3} (Mullin 1969)	Doliolids, copepods, cladocerans, LB-MS, group-specific regressions (Cushing et al 1958)	Calanoid and cyclopoid copepods, cladocerans, LB-MS, group-specific regressions (Gismervik et al. 2002)

of heterotrophs, all according to their functional role and size (Fig. 1). A1 constituted picoplankton (<2- μm equivalent spherical diameter [ESD]), mainly solitary picocyanobacteria. A2 (2–20- μm ESD) and A3 (20–200- μm ESD) consisted of diatoms, dinoflagellates, and other autotrophic flagellates. H1 comprised heterotrophic bacteria including Archaea (<1- μm ESD); H2 comprised heterotrophic nanoplankton (mainly flagellates); H3 comprised microzooplankton dominated by ciliates, rotifers and nauplii; and H4 comprised mesozooplankton, mainly copepods, cladocerans, and doliolids (Table 2).

Biomass was determined on basis of cell counts and biovolume, determined by epifluorescence microscopy (Porter and Feig 1980), image analysis, or flow cytometry (Duarte et al. 2000). The biomass was converted from biovolume to carbon according to carbon to biovolume ratios given in Table 2. The biomass of large zooplankton was also estimated on the basis of counts and length measurement under the microscope, followed by conversion to carbon using group-specific regressions (Table 2).

Samples for determination of dissolved inorganic N (DIN), dissolved inorganic P (DIP), and dissolved organic carbon (DOC) were taken daily or every second day from the integrated water sample after prescreening through 200-

μm nylon nets (<200- μm fraction). DIN and DIP were analyzed immediately after filtration through precombusted (450°C, 4 h), acid-washed (10% HCl) GF/F glass-fiber filters. DOC in the filtrate was analyzed by catalytic high-temperature combustion and infrared detection. POC was collected on precombusted, acid-washed GF/F glass-fiber filters (as for DIN and DIP), and analyzed in CHN (carbon, hydrogen, nitrogen) analyzers. The analytical methods were those commonly used for seawater (Web Appendix 1, http://www.aslo.org/lo/toc/vol_51/issue_1_part2/0488a1.pdf). Detrital carbon (DeC) was calculated as the difference between measured total particulate organic carbon (POC; <200 μm) and total plankton carbon biomass, termed biotic carbon (BiC).

Flow measurements included primary production (measured in three size fractions in BAL and NOR), bacterial production, respiration (MED and BAL, measured in three size fractions in BAL), carbon release (not measured in NOR), sedimentation, and some grazing rates (measured in MED) (Web Appendix 1).

Flow-rate estimation—The simple planktonic food web in Fig. 1 formed the frame for the flow network reconstructions in all experiments. The flows include four or more input terms: primary production by autotrophic groups (A1, A2,

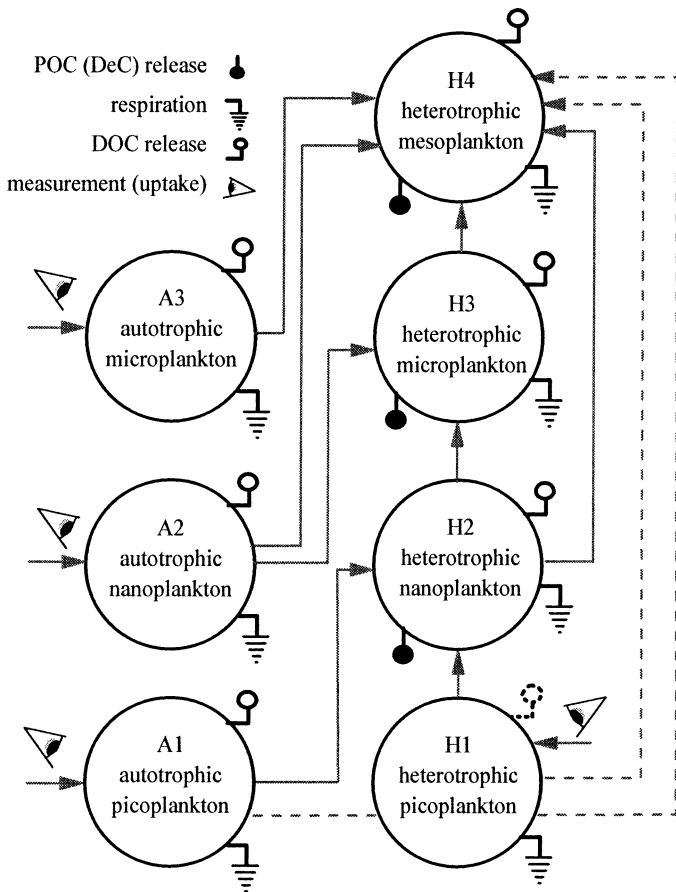


Fig. 1. Generic food web structure and carbon flows forming basis for the carbon flow network constructions. Flows from A1 and H1 to H4 (broken arrows) were only included in MED. Release of DOC from H1 (exudation, excretion, lysis) was included in BAL and NOR (broken symbol). The compartments of DOC and DeC and flows to and from these compartments, including sedimentation of DeC, are not included.

and A3) and uptake of dissolved organic carbon (DOC) by bacteria (H1). Up to 17 output terms expressed the release of DOC from all components, release of detrital particulate organic carbon from heterotrophs (DeC), and respiratory CO_2 from all components. Predation by zooplankton (H2, H3, and H4) was represented by 8 flows in BAL and NOR and 10 flows in MED. In the latter, the doliolid-dominated mesozooplankton (H4) also grazed on picoplankton (A1 and H1; Katechakis et al. 2002). Finally, sedimentation of DeC closed the pelagic mass balance. More flows could have been introduced, but this would have made the results less robust. The inputs included 36–99 measured flows and 90–110 measured stocks for each experiment. All confidence limits given for mean values presented below refer to 1 standard error of the mean (± 1 SE).

A mass balance equation is associated with each flow network compartment, relating the net rate of change to the sums of flows in and out of the compartment. The resulting system of equations is always underdetermined (i.e., more unknowns than equations). Additional equations arise from any measured flow, such as primary production. Solutions,

however, must satisfy a number of a priori inequality constraints that can be derived from general physical and physiological limitations (Web Appendix 2: http://www.aslo.org/lo/toc/vol_51/issue_1_part2/0488a2.pdf). The systems of equations and the inequality constraints were solved for the unknown flows with the Vézina and Platt (1988) algorithm, which yielded constrained minimum norm least square solutions. These will henceforth be called inverse solutions, and the associated vector elements will be termed reconstructed flows.

Net rates of change were estimated from the difference between initial and final values in a quadratic polynomial fitted to the whole time series, augmented with initial measurements from all enclosures (assuming that they started from identical initial conditions). All mass balance equations involved accordingly measured changes; steady state was not assumed in any mass balance.

The key element in the first part of the Vézina–Platt algorithm is a matrix factorization called the singular value decomposition (SVD), one of the most stable numerical methods for solving a least squares problem. The second part applies a least-distance algorithm to a subset of the SVD solution (corresponding to the most significant singular values), such that the inequality constraints are satisfied. Choosing the number of singular values is a problem. Although it would be natural to use the rank of the equation system if the measurements were error free, this is seldom possible. Vézina and Platt (1988) recommended graphing the solution and the residual norms for different numbers of singular values and choose the one closest to the curve intersection. In our experience, the inversion algorithm is often unable to find a solution when the number of singular values is close to the rank of the system. Unfortunately, this can only be detected by substituting the solution into the original constraints (which will then be violated). We have therefore included as a default approach a linear search for the highest rank solution that satisfies the constraints. The measured rates (Table 3) were used to check the goodness of fit of the flow rate estimated by the inverse problem solution procedure. We used Matlab software (MathWorks) for our implementation of the Vézina–Platt algorithm.

Results

The average concentration of DIN was high at the highest nutrient input rates (L_N) in MED and NOR mesocosms, but not in BAL, which also showed the lowest concentrations (Fig. 2A). DIP accumulated with increasing L_N in BAL and NOR and at the highest rate of nutrient input in MED (Fig. 2B). Generally, accumulation of DIN and DIP was temporary, occurring during the first week of the experiments (not shown). The overall variation in nutrients suggest that on average, the phytoplankton of MED mesocosms was potentially P limited, that of BAL was potentially N limited, and that of NOR was N limited, but close to the Redfield ratio.

The functional planktonic groups A1, H1, and H2 contained to great extent the same main taxonomic groups of organisms in the three locations, whereas the species/group composition of A2, A3, H3, and H4 was highly diverse (Ta-

Table 3. Linear regression of carbon biomass and gross carbon uptake of autotrophic and heterotrophic components versus nitrogen loading rate (L_N , i.e., slope of regression, r^2 , in parentheses). Significance level: ns, $p > 0.05$; * $p < 0.05$; ** $p < 0.01$; *** $p < 0.001$.

	Location		
	BAL	MED	NOR
Biomass of component			
A1	0.50±1.25 (0.026) ns	0.37±0.15 (0.68) *	-0.62±6.20 (0.002) ns
A2	105±14 (0.91) ***	0.29±0.28 (0.26) ns	266±30 (0.94) ***
A3	440±73 (0.86) ***	4.79±1.79 (0.71) *	89±16 (0.86)
H1	4.72±0.91 (0.82) ***	1.38±0.34 (0.85) *	7.51±1.76 (0.78) **
H2	-2.29±4.09 (0.05) ns	0.19±0.20 (0.23) ns	2.28±0.82 (0.61) *
H3	16.0±2.7 (0.85) ***	0.064±0.013 (0.89) **	10.2±1.4 (0.91) ***
H4	6.28±6.15 (0.15) ns	0.13±0.59 (0.02) ns	3.27±5.01 (0.08) ns
DeC	150±83 (0.35) ns	31.1±10.8 (0.73) *	130±18 (0.91) ***
Sum A	575±86.2 (0.88) ***	5.46±2.19 (0.675) ns	360±46.6 (0.923) ***
Sum H	25.9±6.79 (0.708) **	1.78±0.25 (0.946) **	23.1±8.31 (0.606) *
Sum A : Sum H	5.79±1.30 (0.767) **	0.144±0.086 (0.481) ns	2.61±0.37 (0.909) ***
Gross carbon uptake/ingestion			
GPP of A1	2.42±3.31 (0.082) ns	1.16±1.35 (0.197) ns	11.4±2.24 (0.836) **
GPP of A2	101±8.08 (0.963) ***	13.6±4.34 (0.765) ns	148±5.2 (0.994) ***
GPP of A3	144±13.1 (0.953) ***	14.2±4.30 (0.784) *	25.3±4.99 (0.837) **
GHU of H1	24.3±9.69 (0.511) *	9.32±1.38 (0.938) **	45.6±4.90 (0.945) ***
GHU of H2	4.02±4.69 (0.109) ns	3.01±1.65 (0.526) ns	14.5±0.85 (0.983) ***
GHU of H3	33.9±4.74 (0.895) ***	0.47±1.43 (0.035) ns	46.6±0.87 (0.998) ***
GHU of H4	32.7±8.53 (0.710) **	16.7±3.97 (0.855) *	48.7±1.94 (0.992) ***
DeC formation	23.2±15.9 (0.264) ns	3.30±5.50 (0.107) ns	87.1±2.93 (0.994) ***
GPP of Sum A	235±16.0 (0.973) ***	28.9±9.55 (0.753) ns†	181±6.8 (0.993) ***
GHU of Sum H	70.6±12.0 (0.853) **	20.2±6.89 (0.741) ns‡	110±2.5 (0.997) ***

† $p = 0.0566$.

‡ $p = 0.0611$.

ble 2). The initial biomass of the food web components differed greatly between the sites (Fig. 3A and BiC in Fig. 3B). Thus, the oligotrophic MED waters exhibited the lowest biomasses of all components except for H4. The initial biomass of BAL and NOR waters were higher and similar, but the initial H4 mesozooplankton biomass was particularly low in BAL. Initial particulate DeC (Fig. 3B) was high and similar in MED and BAL and somewhat lower in NOR. DOC was the main component of organic C in all systems, and the initial values of DOC and total C were far higher in BAL than in MED and NOR (Fig. 3C).

The biomass of most of the functional components, including DeC, responded positively to enhanced nutrient input rate (Fig. 4), but 9 out of 24 components did not respond significantly ($p > 0.05$; Table 3). Most of the components showed a stronger response to increased L_N in BAL and NOR mesocosms than in MED, in particular the eukaryotic phytoplankton (A2 and A3), which accumulated little in MED. A1 biomass, however, responded slightly yet significantly to enhanced nutrient input only in MED. The biomass of A3, H1, and H3 responded significantly in all experiments, whereas the response of H4 was insignificant ($p > 0.05$). Copepods, which dominated H4 of the NOR communities, did respond to nutrient addition, but most strongly at intermediate nutrient loadings. This may be a consequence of inappropriate nutrition quality of the diatoms (Nejstgaard et al. 2001; Gismervik et al. 2002).

The gross primary production (GPP) and gross heterotrophic uptake (GHU) increased significantly with increasing

L_N for 15 out of 21 plankton components and DeC formation increased significantly in NOR (Fig. 5; Table 3). GPP of A1 responded relatively weakly compared to GPP of the other autotrophs in all experiments, and the group responded weakly significantly in NOR (Table 3). GPP of A3 increased significantly in all experiments ($p < 0.05$).

GHU by H1 (i.e., DOC uptake) increased significantly with increasing nutrient inputs in all communities ($p < 0.05$). BAL exhibited the highest uptake rates, but the strongest response to increased L_N was found in NOR (Table 3). GHU of most zooplankton groups (H2–H4; i.e., C-ingestion rates) increased with increasing nutrient input in all NOR communities, but only sporadically in BAL and MED (Fig. 5; Table 3). A2 phytoplankton was the main food source for ciliates in BAL and NOR communities (see Web Appendix 3, http://www.aslo.org/lo/toc/vol51/issue_1_part2/0488a3.pdf). Mesozooplankton (H4) consumed mainly A2 and A3 and also small quantities of H3 in BAL and NOR.

It is noteworthy that both the feeding and biomass responses of H3 in MED were insignificant (Fig. 3). H4 was the main consumer in MED, exceeding the grazing rate of the protozoa (H2 and H3) by a factor of 5. The H4 zooplankton had access to picoplankton in MED, but not in BAL and NOR (Fig. 1), because doliolids which dominated H4 in MED feed on a broad spectrum of food sizes, including picoplankton (Katechakis et al. 2002). Nanoheterotrophs (H2), however, still were the main consumers of picoplankton (A1 and H1) in all experiments (Web Appendix 3).

The accumulation of autotrophic (SumA or A) and het-

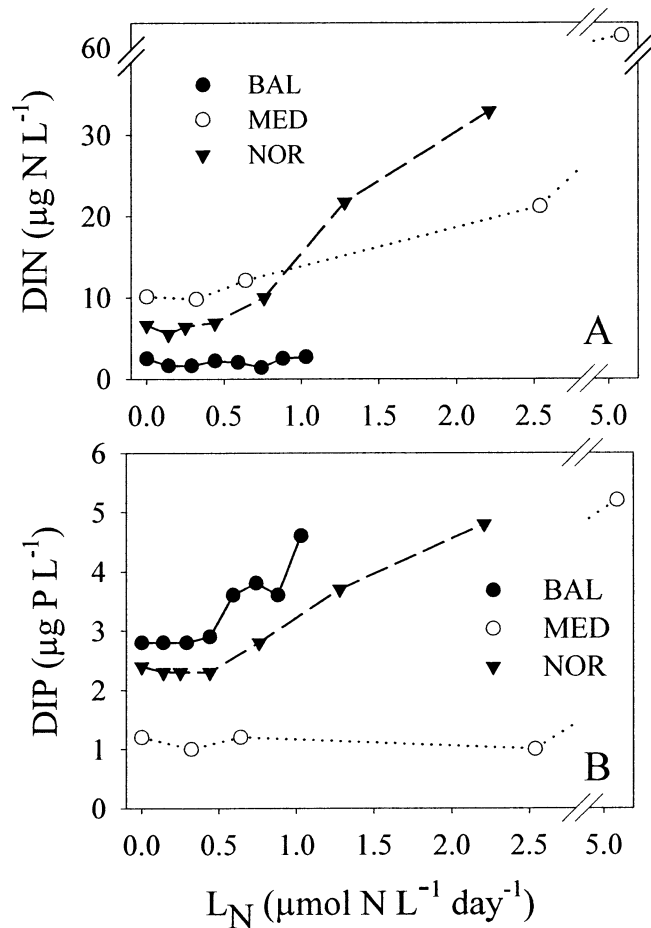


Fig. 2. (A) Average concentration of DIN and (B) DIP in BAL, MED, and NOR mesocosms as a function of nitrogen loading rate (L_N) of the mesocosms. Loading rates of P and Si were proportional to those of N (Redfield proportions; Table 1).

erotropic (SumH or H) biomass was far lower in MED than in BAL and NOR, which showed similar and highly significant biomass responses (Fig. 6A,B; Table 3). Autotrophic biomass accumulation was insignificant ($p > 0.05$) in MED, but the heterotrophic biomass increased significantly with increasing L_N ($p < 0.01$; Table 3). All response curves showed a roughly linear response at nutrient input rates $< 1 \mu\text{mol N L}^{-1} \text{ d}^{-1}$.

In MED, the ratio A:H stayed < 1 even at the highest rate of nutrient input while increasing by almost one order of magnitude with increasing L_N in BAL and NOR (Fig. 6E). This suggests a consistently higher grazing pressure over the whole range of nutrient input in MED than in BAL and NOR.

The response of total GPP and total GHU to increasing nutrient input differed less between the sites than the response in biomass (Fig. 6C,D). Thus, GPP was consistently higher in BAL than in MED and NOR, yet all communities showed a similar linear response at input rates < 0.7 – $1 \mu\text{mol N L}^{-1} \text{ d}^{-1}$. Moreover, there was no obvious and systematic difference in total GHU between the systems for $L_N < 1 \mu\text{mol N L}^{-1} \text{ d}^{-1}$. The variability and the low number of flow estimates in the higher range of nutrient input rates (> 1

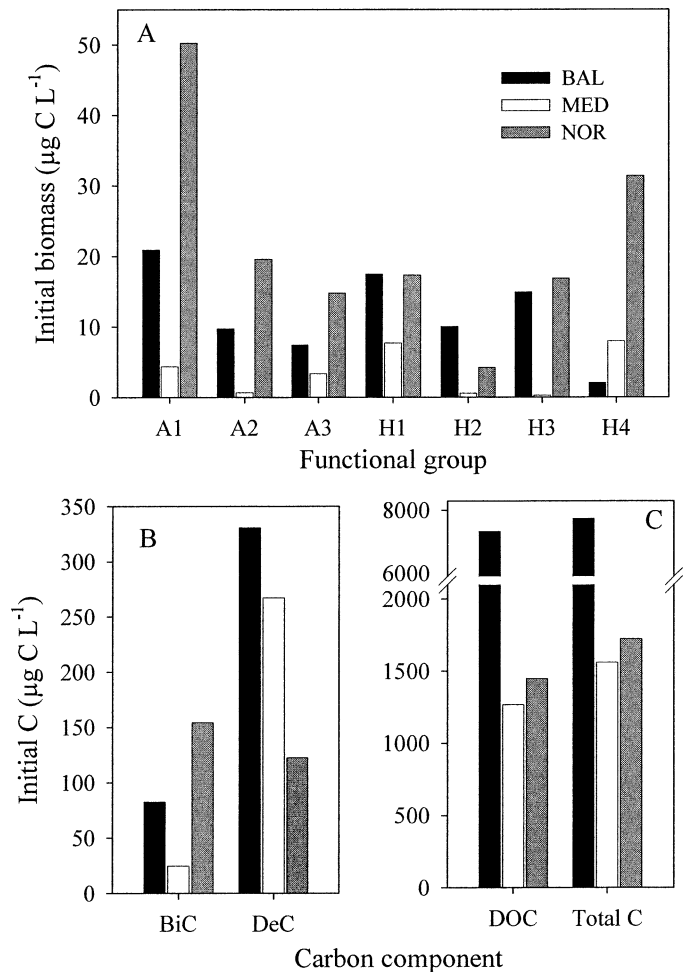


Fig. 3. (A) Initial carbon biomass of functional groups and (B, C) biotic and abiotic organic carbon components in BAL, MED, and NOR mesocosms (organisms in Table 2).

$\mu\text{mol N L}^{-1} \text{ d}^{-1}$) makes comparisons and generalization about GPP and GHU at high nutrient input impossible. The low GPP of the MED community for high L_N was most likely a consequence of the lack of biomass accumulation.

GHU was consistently lower, but of same magnitude as GPP. The GHU:GPP ratio decreased with increasing nutrient input rate (Fig. 6F) in all systems, with the generally highest values for MED, in agreement with the high grazing pressure.

Pooled data for all three locations reveal a remarkably consistent linear pattern of increase in the total zooplankton grazing rate as a function of GPP (Fig. 7A; Table 4). The H4 ingestion rate in MED averaged $43\% \pm 7\%$ of the autotrophic production, as compared to $21\% \pm 3\%$ and $18\% \pm 2\%$ in BAL and NOR, respectively (not shown). The importance of autotrophic food for the zooplankton increased with increasing GPP in all systems. The fraction of autotrophic food was lowest in MED and highest in NOR (Fig. 7B).

The release of DOC by autotrophs increased with increasing GPP in all systems (Fig. 7C), and the released fraction was higher in the MED communities ($p < 0.01$, $24\% \pm 3\%$

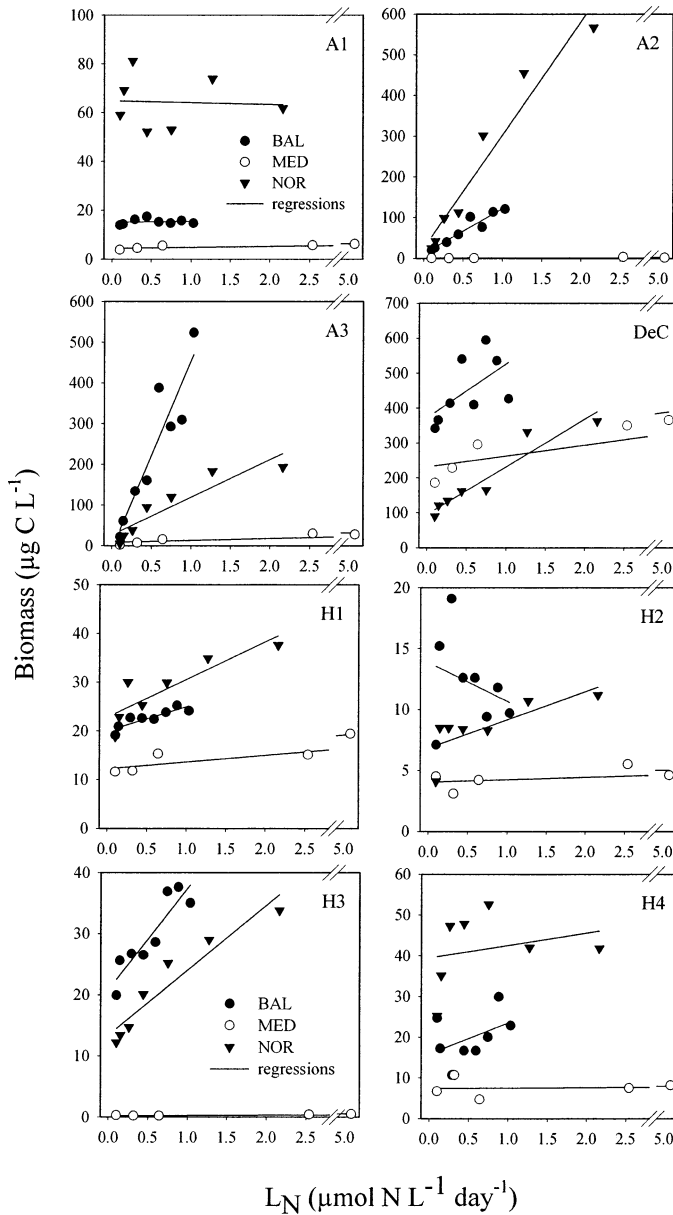


Fig. 4. Average biomass of autotrophic and heterotrophic functional groups in BAL, MED, and NOR mesocosms as a function of the nitrogen loading rate of the mesocosms (L_N ; Table 1). The curves express regression lines.

of GPP), as compared to BAL and NOR ($13\% \pm 2\%$ and $9.6\% \pm 3.5\%$ of GPP, respectively). The DOC release rate by heterotrophs was generally higher than the DOC release rate for autotrophs in the NOR and BAL communities. MED heterotrophs, in contrast, exhibited very low release rates of DOC (Fig. 7D). The release rate of POC by the zooplankton (DeC, H2–H4) showed a significant and similar linear increase with increasing GPP in all systems ($p < 0.0001$, $r^2 = 0.627$; Fig. 7E). The mean DeC release flow from zooplankton corresponded to $20\% \pm 2\%$ of GPP.

The community respiration rate was also linearly related to GPP (Fig. 7F; Table 4) and exceeded GPP for $GPP < 51 \mu\text{g C L}^{-1} \text{d}^{-1}$, suggesting that the coastal communities

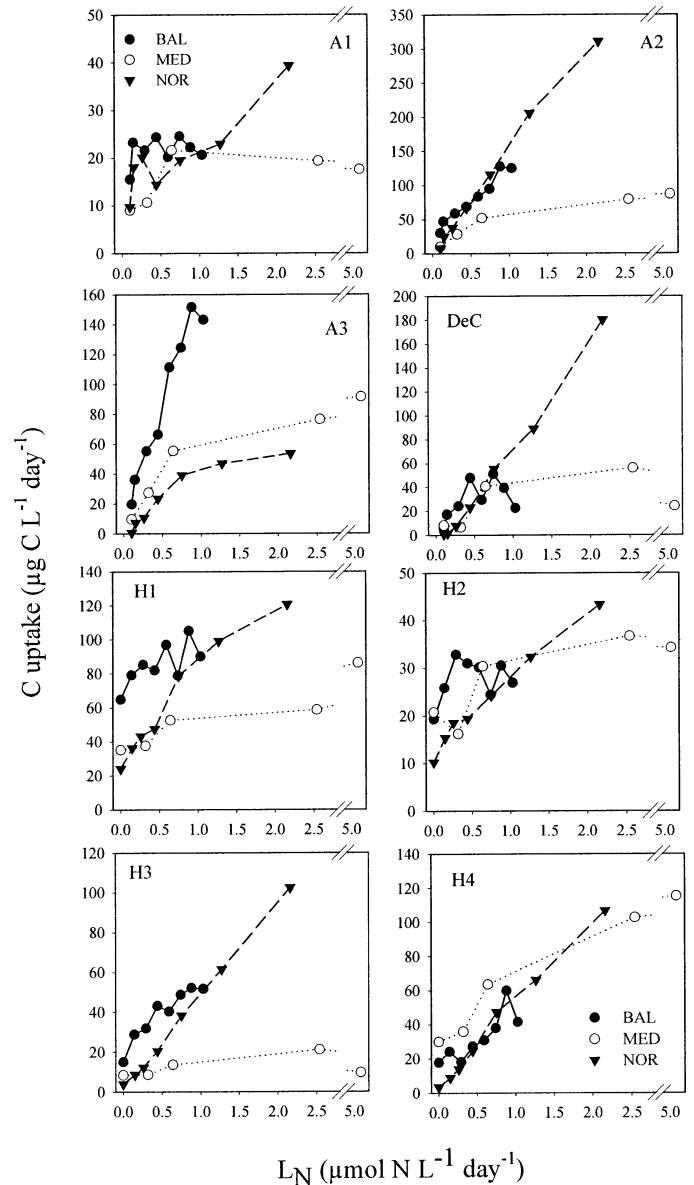


Fig. 5. Average carbon uptake rates of autotrophic and heterotrophic functional groups in BAL, MED, and NOR mesocosms as a function of the nitrogen loading rate of the mesocosms (L_N ; Table 1).

should be net heterotrophic for lower GPP. Communities showing higher GPP, i.e., those with loading rates of about $0.15 \mu\text{mol N L}^{-1} \text{d}^{-1}$ (range $0\text{--}0.25 \mu\text{mol N L}^{-1} \text{d}^{-1}$; Fig. 6C), would therefore be net autotrophic.

Carbon uptake by the bacteria (H1) was linearly and equally related to GPP in all systems (Fig. 8A). The y-intercept of the regression curve ($32.7 \pm 5.1 \mu\text{g C L}^{-1} \text{d}^{-1}$) was significantly >0 ($p < 0.0001$), indicating a positive DOC uptake by H1 for zero GPP. GPP exceeds DOC uptake by H1 for $GPP > 43 \mu\text{g C L}^{-1} \text{d}^{-1}$ (Table 4).

There was a general and common linear relationship between the total community DOC release rate and the total carbon uptake by H1 bacteria (slope 0.749 ± 0.0372 , $p < 0.0001$, $r^2 = 0.957$; Fig. 8B). DOC uptake of H1 was sig-

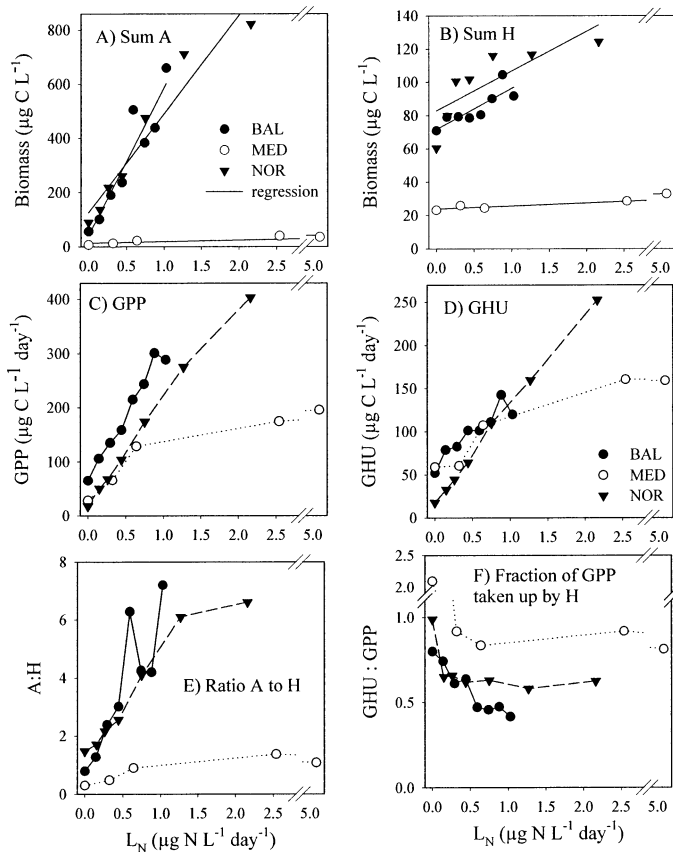


Fig. 6. Average biomass, carbon uptake rates, and ratios between autotrophs and heterotrophs biomass and activity in BAL, MED, and NOR mesocosms as a function of the nitrogen loading rate of the mesocosms (L_N ; Table 1). (A) Total autotrophic biomass; (B) total heterotrophic biomass; (C) total carbon uptake in autotrophs or gross primary production (GPP); (D) total carbon inflow in heterotrophs or gross heterotrophic uptake (GHU); (E) total autotrophic to heterotrophic biomass (A:H ratio); (F) total GPP to total GHU ratio.

nificantly >0 for zero food web release of DOC (15.5 ± 3.0 , $p < 0.0001$).

The growth efficiency (GE) of all heterotrophic groups was inversely related to L_N in NOR and for H2 and H4 in MED, but was significant only for H4 in NOR ($p < 0.01$; Table 5). The GE values, however, were positively related to nutrient input in BAL. The growth efficiency equaled the constraining conditions only for H1 and H3 in MED. The only negative GE value was for H4 in BAL (Web Appendix 2).

A summary of the biomass response (Fig. 9) shows that

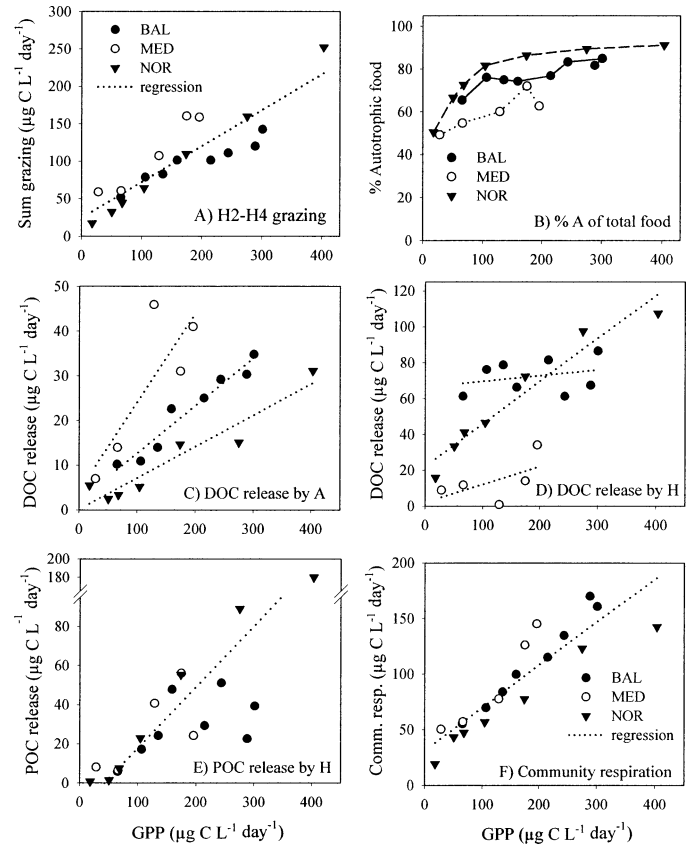


Fig. 7. Zooplankton- (H2-H4) mediated carbon flows in BAL, MED, and NOR mesocosms as a function of gross primary production (GPP). (A) Grazing rate; (B) the zooplankton fraction of autotrophic food; (C) total DOC release by autotrophs; (D) total DOC release by zooplankton; (E) DeC (POC) release by zooplankton; (F) total community respiration rate.

nanoautotrophs (A2) and microautotrophs (A3) exhibit stronger response to nutrient additions than any other component (Fig. 9, first column of graphs). The far smaller biomass and response of MED communities illustrate that the biomass yield per unit of nutrient input is fundamentally different in MED compared to BAL and NOR. Picocyanobacteria (A1), initially the dominating autotrophs in all communities, became unimportant at high nutrient input.

The heterotrophic components showed no or a moderate response during the 2-3 weeks of increased nutrient input (Fig. 9, second column). Bacteria (H1) dominated heterotrophic biomass in the MED mesocosms, whereas in BAL and NOR this group dominated together with microzooplankton (H3, mainly ciliates) and mesozooplankton (H4). The initial

Table 4. Linear regression coefficients describing zooplankton grazing (H2-H4) and bacterial activity (H1) as a function of GPP of pooled BAL, MED, and NOR data.

Relationship	Slope	Intercept $\mu\text{g C L}^{-1} \text{ day}^{-1}$	r^2	p
Total grazing by H2-H4 versus GPP	0.479 ± 0.056	24.2 ± 10.6	0.804	<0.0001
Autotroph grazing by H2-H4 versus GPP	0.462 ± 0.042	3.55 ± 7.87	0.872	<0.0001
Community respiration versus GPP	0.385 ± 0.043	31.4 ± 8.10	0.817	<0.0001
DOC uptake by H1 versus GPP	0.234 ± 0.027	32.7 ± 5.11	0.806	<0.0001

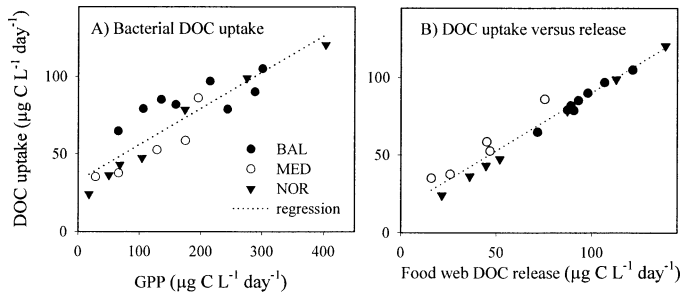


Fig. 8. Bacterial (H1)-mediated carbon uptake in BAL, MED, and NOR mesocosms as a (A) function of GPP and (B) total food web DOC release.

ratio of autotrophs to heterotrophs (A : H) varied from 0.3 to 1.5, with the lowest values in MED (Fig. 9, third column). The ratio increased almost one order of magnitude for high L_N in BAL and NOR waters, while leveling off close to unity in MED.

Particulate detrital carbon (DeC) clearly dominated particulate organic carbon (POC = BiC + DeC) in MED (Fig. 9, fourth column), and concentrations were generally lower than in BAL and NOR. The biotic components (BiC) dominated in NOR, which also showed the strongest response in total POC. BiC and DeC concentrations were comparable in BAL, but the response to increased nutrient input was most consistent for BiC.

The estimation of BiC, and therefore also DeC, regrettably involves major uncertainties. Systematic errors, which may differ for the sites, may accumulate through counting, bio-volume determination, and conversion to carbon biomass. The general patterns of variation found for BiC and DeC among sites will not, however, be seriously affected by such errors (Fig. 9). The main pattern of variation is believed to be relatively robust to these systematic errors involved in biomass determination of the single groups.

DOC was by far the most important pool of organic carbon in all types of coastal waters, and DOC concentrations in BAL were far higher than in NOR and MED. DOC con-

centrations were comparable in MED and NOR waters despite the much lower biomass of biotic components of the MED communities.

Unlike autotrophic biomass accumulation, GPP of autotrophs was of the same magnitude in all systems (Fig. 10, first column). Both A2 and A3 became dominant primary producers in the nutrient enriched BAL and MED communities, while A2 became dominant in NOR. A significant response in GPP of A1 with increasing nutrient input was only found in NOR. The allocation of carbon to net growth, respiration, and release of DOC was similar in all systems, but the relative proportion of released DOC was highest in MED (Fig. 10, third column). Of the carbon uptake of autotrophs (SumA), 42–72% was retained in new biomass in all systems for all nutrient input rates, 17–42% was respired, and 5–36% was released as DOC.

Gross carbon uptake and grazing rates of the heterotrophic groups (GHU) showed comparable flows in all systems (Fig. 10, second column). Responses were generally moderate and variable in BAL. Bacterial (H1) uptake rate, and particularly the mesozooplankton (H4) grazing rate, responded in MED. The gross carbon uptake of all heterotrophic groups increased in NOR. Of the carbon uptake of the heterotrophs (SumH), 7–44% was retained in new biomass across all systems and nutrient input rates, 16–47% was respired, 1–52% was released as DOC, and 2–48% was released as DeC (Fig. 10, fourth column). Heterotrophic MED plankton showed the highest efficiency of carbon allocation into biomass, highest losses through respiration, and lowest losses of DOC. BAL and NOR were similar in terms of carbon allocation.

Discussion

Although pelagic mesocosms are useful tools for studying short-term effects of nutrient perturbation of planktonic communities, extrapolation from our experiments to natural systems is not straightforward. The effect of anthropogenic coastal eutrophication cannot easily be experimentally sim-

Table 5. Estimated gross growth efficiencies (%GE; $g/i \times 100$) of heterotrophic groups. Ingestion (i) is the gross carbon uptake in H1 or food ingestion in H2–H4; growth (g) is estimated as Ingestion – Respiration – DOC release – DeC release. POS, positive correlation between L_N and %GE; NEG, negative correlation L_N and %GE; ns, $p > 0.05$; **, $p < 0.01$; n equals numbers of mesocosm units.

Location	Parameters	Group			
		H1	H2	H3	H4
BAL (n=8)	Mean±1 SE	22.3±1.1	11.2±1.3	10.3±0.2	6.7±1.8
	Range	(18.1–27.1)	(9.7–20.3)	(9.9–11.9)	(–2.1–15.0)
	Correlation	POS/ns	POS/ns	POS/ns	POS/ns
MED (n=5)	Mean±1 SE	60±0*	32.4±2.6	10±0†	28.0±4.6
	Range		(25.0–38.5)		(14.8–42.4)
	Correlation		NEG/ns		NEG/ns
NOR (n=7)	Mean±1 SE	17.6±0.8	19.1±5.4	11.0±0.7	8.2±1.9
	Range	(14.3–20.4)	(9.9–49.0)	(9.9–15.4)	(0.7–17.1)
	Correlation	NEG/ns	NEG/ns	NEG/ns	NEG/**
All locations (n=20)	Mean±1 SE	30.1±4.0	19.0±2.7	10.5±0.3	12.6±2.5
	Range	(14.3–60)	(9.7–49.0)	(9.9–15.4)	(–2.1–42.4)

* Values equal to upper constraint value; see Web Appendix 2.

† Values equal to lower constraint value; see Web Appendix 2.

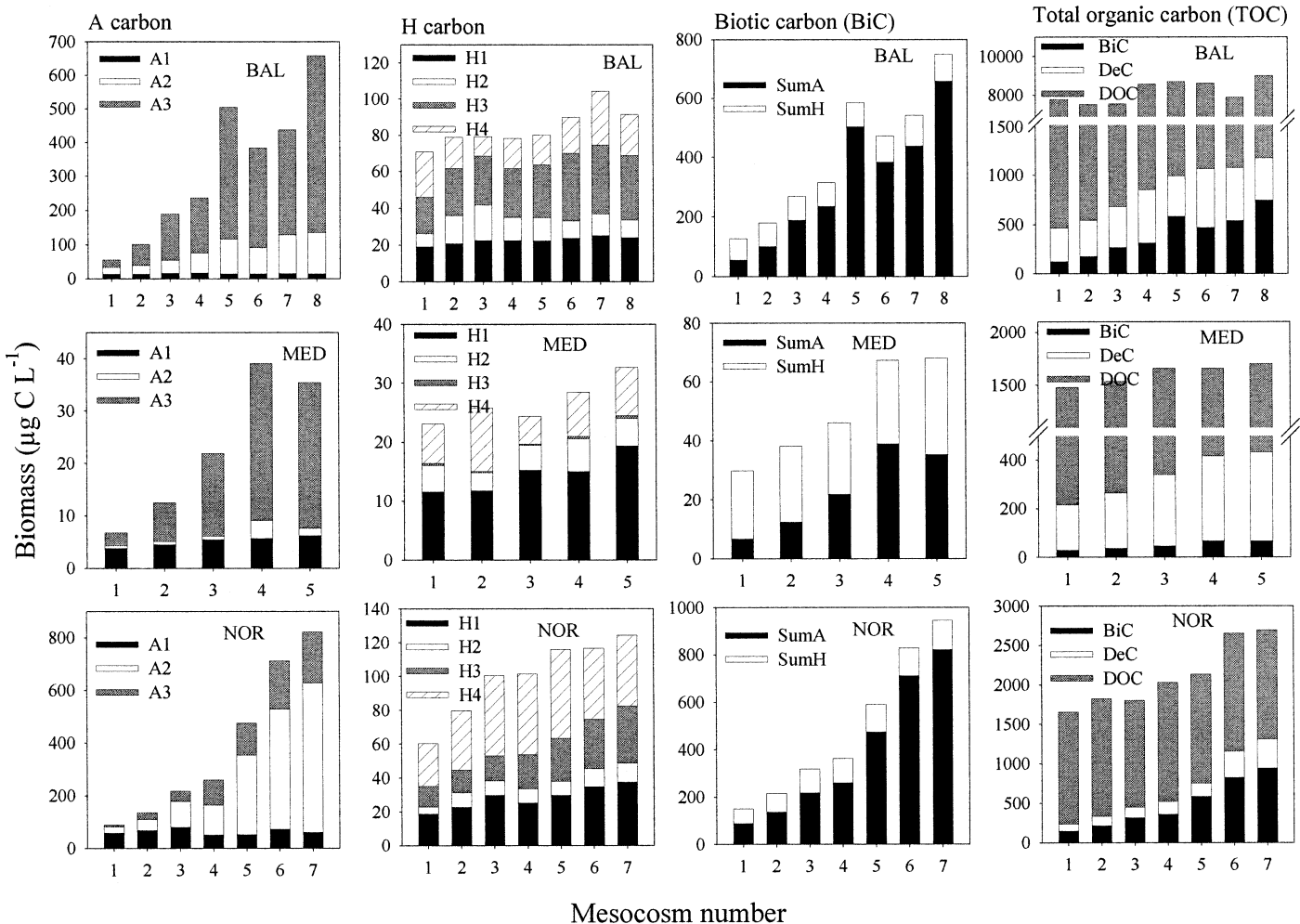


Fig. 9. Summary of biomass responses and abiotic carbon components in BAL, MED, and NOR mesocosms added variable doses of nutrients (L_N ; Table 1). First column: autotrophic biomass; second column: heterotrophic biomass; third column: total autotrophic (SumA) and heterotrophic (SumB) biomass (biotic, BiC); fourth column: biotic (BiC) and abiotic organic carbon components (DeC and DOC) (note different y scale of MED compared to BAL and NOR; predominant organisms in Table 2).

ulated. Experiments of 2–3 weeks' duration will, for example, describe transient responses because the larger zooplankton and their direct and indirect predation effect will be realized in full only over longer time scales (Gismervik and Andersen 1997; Gismervik et al. 2002; Vadstein et al. 2004; see following). It is also important that only species initially present can respond in a closed mesocosm experiment. This is but one problem of the validity of results obtained in short-term mesocosm experiments.

The inverse method allows simultaneous estimation of all major food web flows, some of which cannot be easily measured. The method is simply a consistent and standardized procedure for determining the mass balance between the components of the food web and its surroundings. The calculated flows can be biased, however, to an extent partly unknown because of the underdetermined set of equations and because the trophic structure and the flow constraints obviously are too simple. Our treatment rests on the assumption that any bias should apply uniformly, thus allowing cross-system comparisons. Importantly, the calculations,

which treat each mesocosm independently, yielded high-rank solutions that generally formed a uniform pattern with increasing nutrient input rate for all three experiments.

The species composition of the functional groups (Table 2; Fig. 1) showed major differences for the regional coastal communities, yet relatively consistent patterns were found in the responses of most of the functional components and gross uptake flows. This pattern consistently comprised a linear increase of biomass and uptake flows with increasing nutrient input rate in the lower range of input rates ($<1 \mu\text{mol N L}^{-1} \text{d}^{-1}$). Another striking feature was the far lower accumulation of autotrophic (A2 and A3 phytoplankton) biomass at high nutrient input in the MED mesocosms than in BAL and NOR. A third major observation was the relatively uniform abundance and low response of picocyanobacteria (A1) at all locations.

The autotrophic biomass in MED was surprisingly little affected by nutrient addition. The higher nutrient input rates for MED than for BAL and NOR (Table 1) were in fact chosen based on preliminary tests that revealed this low re-

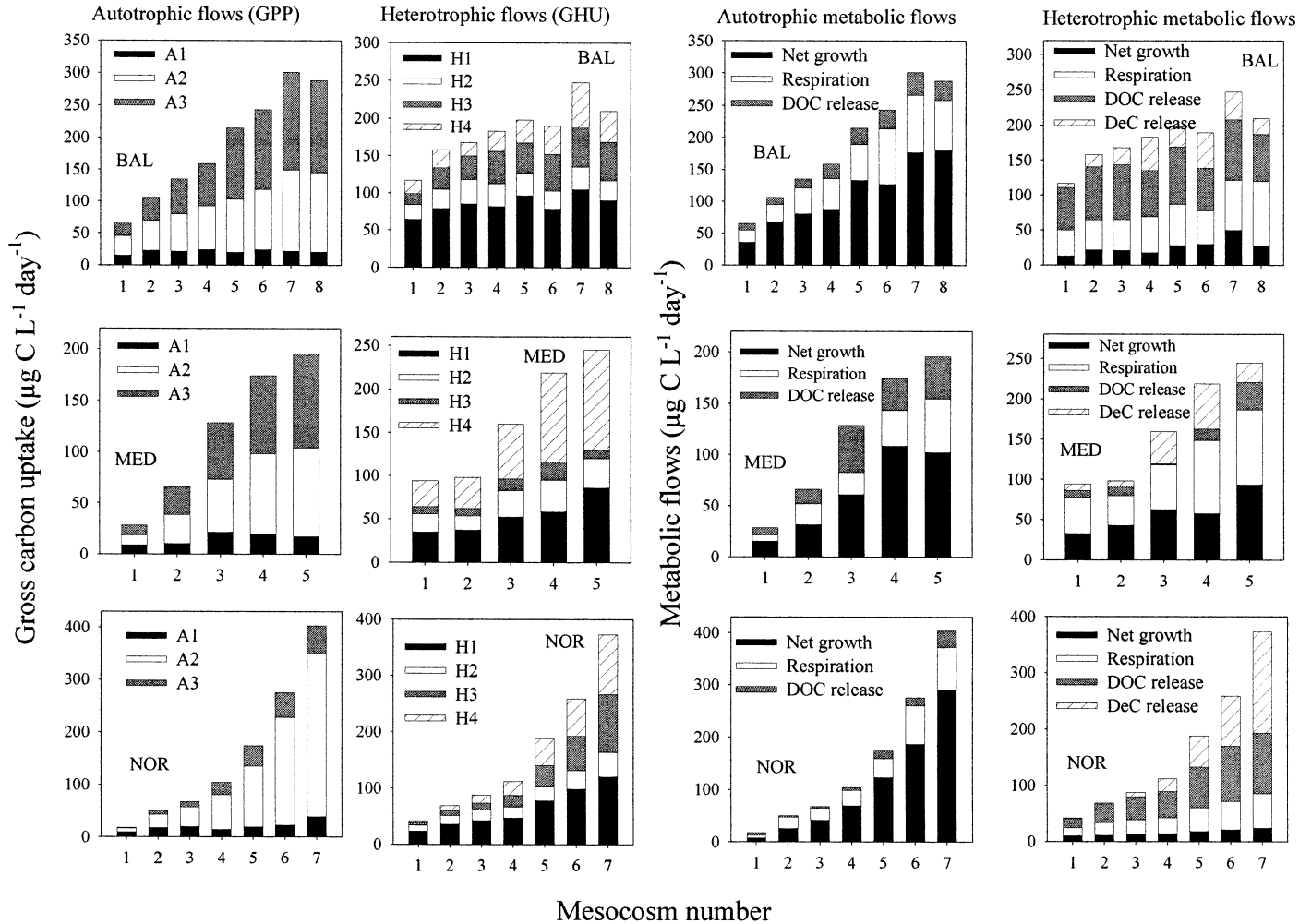


Fig. 10. Summary of responses in gross carbon uptake and metabolic carbon flows in autotrophic and heterotrophic groups in BAL, MED, and NOR mesocosms with variable doses of added nutrients (L_N ; Table 1). First column: gross primary production (GPP) of autotrophic groups; second column: gross heterotrophic uptake (GHU) of heterotrophic groups; third column: net growth, respiration, and DOC release flows of total autotrophs; fourth column: net growth, respiration, and DOC release flows of total heterotrophs (predominant organisms in Table 2).

sponse. The absence of biomass accumulation in the MED mesocosms was not caused by a low primary production because GPP of the autotrophic groups in MED responded in a fashion comparable to BAL and NOR (Figs. 5, 6). In fact, total GPP showed the same quantitative relationship with L_N in the lower range of nutrient input rates ($<1 \mu\text{mol N L}^{-1} \text{d}^{-1}$) for all sites. Yet the nutrients added to MED were effectively removed from the water and the photosynthetic activity responded to the nutrient addition. The autotrophic biomass, in contrast, did not accumulate.

According to Agustí and Duarte (2000), the very small biomass response of MED phytoplankton to nutrient addition was accompanied by an apparently high phytoplanktonic lysis rate. Our data, however, suggest that efficient grazing by H4 was the principal factor counteracting phytoplankton blooms in MED. The initial H4 biomass was relatively high (Fig. 3), and the doliolids that dominated H4 were capable of consuming most of the small-sized plankton groups (Katchakis et al. 2002). Although the grazing activity in-

creased, the biomass of H4 did not increase significantly with increasing nutrient input (Fig. 5; Table 3). The higher grazing pressure in MED than in BAL and NOR was also reflected by a consistently lower and nonresponsive A:H ratio ($p = 0.48$ for A:H vs. L_N in MED; Table 3). While H4 ingestion rate in MED averaged $43\% \pm 7\%$ of the autotrophic production, it averaged $21\% \pm 3\%$ and $18\% \pm 2\%$ in BAL and NOR, respectively.

The reduction in GPP in the most strongly fertilized MED mesocosms (Fig. 6C) is in good agreement with strong grazing control. The suppression of phytoplankton biomass limits carbon assimilation to the extent that it became limited by the maximum specific growth rate of the autotrophs. The specific growth rate of these MED mesocosms (net PP \times biomass $^{-1}$) was 2.8–2.9 d^{-1} , very high for temperatures of 19–21°C.

It is widely accepted that the initial structure of the planktonic food web in mesocosm experiments to some extent will have an effect on the final results. Our arrangement of the

species into functional groups probably reduced the importance of initial species composition because species within each particular functional group would perform similar ecological roles in the ecosystem. It is nevertheless very likely that the high initial biomass and the dominance of doliolids in MED might have been important for the later grazing control during the nutrient perturbations. Predominance of copepods in MED could have caused a completely different succession. We believe that the results for BAL and NOR are fairly representative for the summer–autumn situation in these locations, implying that nutrient input would normally yield an increase in the phytoplankton biomass.

Although differing among localities, the picocyanobacteria predominant in A1 generally formed the dominant autotrophic group initially (Fig. 3A), but increased nutrient input resulted in structural changes. Their GPP was similar to that of A2 and A3 at low L_N (Figs. 4, 5), suggesting that picocyanobacteria were important at all locations (Lignell 1990; Agawin et al. 1998). The picocyanobacteria, however, responded weakly following the increasing nutrient input, never becoming predominant in fertilized communities. This is compatible with the suggestion that picocyanobacteria are fairly nutrient sufficient at the ambient nutrient concentration (Moutin et al. 2002), and therefore controlled mainly by grazing or viral infection (Fuhrman 1999). The small variation in the response pattern of the picocyanobacteria among locations might support recent findings that unicellular cyanobacteria in the open ocean, previously called *Synechococcus* (3–10 μm), may be capable of assimilating atmospheric nitrogen (Zehr et al. 2001). We found no significant response in either biomass or GPP of picocyanobacteria in the N-limited BAL phytoplankton. In the N-limited or nutritionally balanced NOR phytoplankton, GPP responded, but not biomass. In contrast, a small response was evident in both biomass and GPP (lower range of nutrient input) in the P-limited MED phytoplankton (Table 3).

Our results reveal a consistent pattern for the utilization of the primary production by zooplankton and bacteria in the three different coastal food webs (Figs. 7, 8; Table 4). Grazing rates of the heterotrophic zooplankton, carbon uptake rates of the bacteria, the release rates of dissolved and particulate carbon by heterotrophs, and community respiration rates were all linearly related to GPP in the entire range of 10–400 $\mu\text{g C L}^{-1} \text{d}^{-1}$. Moreover, we observed a similar response pattern for all locations in terms of allocation of the consumed carbon of heterotrophs to new growth, respiration, and defecation (i.e., DOC and DeC release; Fig. 10). There were differences among the heterotrophic functional groups in the three locations, but ranges in total heterotrophic uptake and metabolism were similar. The observed differences in metabolic carbon allocation between groups and locations are revealed by the estimated average growth efficiencies of carbon and their range of variation (Table 5). The estimated GE values for all heterotrophic groups were in agreement with data from the literature (Straile 1997; Nagata 2000). Estimates that hit the constraint value in two cases should be judged with care.

The relationship between community respiration and GPP (Fig. 7F; Table 4) was similar to that previously derived from comparative analyses of planktonic communities (Duarte

and Agustí 1998). This study interpreted communities with $\text{GPP} < 50 \mu\text{g C L}^{-1} \text{d}^{-1}$ as net heterotrophic, and our critical value of $51 \mu\text{g C L}^{-1} \text{d}^{-1}$ (Table 4) was indeed very close. Thus, communities receiving very small nutrient inputs ($0.15 \mu\text{mol N L}^{-1} \text{d}^{-1}$, range $0\text{--}0.25 \mu\text{mol N L}^{-1} \text{d}^{-1}$) tended to be temporarily heterotrophic, partially depending on the amount of DOC stored in the system or derived from allochthonous sources. This is consistent with the finding that consumption of DOC by bacteria can exceed GPP in unproductive communities ($< 40 \mu\text{g C L}^{-1} \text{d}^{-1}$; del Giorgio et al. 1997).

The average percent DOC release of GPP by autotrophs among communities and nutrient inputs ($14\% \pm 2\%$, range 6–36%, $n = 20$) was in good agreement with the average of 13% for contrasting ecosystems compiled by Baines and Pace (1991) and 10–20% compiled by Nagata (2000). This DOC flow, however, was insufficient to satisfy the requirements of bacteria. Our results suggest that heterotrophs were responsible for two-thirds of the total DOC production by the food web. Moreover, the food web DOC production rate was closely correlated to the DOC taken up by the bacteria (Fig. 8B; slope of curve 0.749 ± 0.0372 , $p < 0.0001$). Notably, the bacteria assimilated more DOC than the amount released by the food web below a DOC release rate of $62 \mu\text{g C L}^{-1} \text{d}^{-1}$ and less than that above this value. This suggests that the DOC concentration will be reduced at small nutrient input. Carbon must therefore partially be derived from external sources, from accumulated DOC from past algal blooms or from allochthonous DOC inputs. Conversely, during high nutrient inputs and high DOC production, the bacterial demand can be exceeded, leading to an accumulation of DOC (Williams 1995).

Three main conclusions emerge from our experiments. First, in all communities, the gross carbon uptake rate in autotrophic and heterotrophic plankton increased linearly with increasing L_N in the lower range of nutrient input rates ($< 1 \mu\text{mol N L}^{-1} \text{d}^{-1}$). The rate of increase was similar at the three locations. Second, the autotrophic and heterotrophic biomass in all communities increased linearly with increasing L_N in the lower range of nutrient input rates ($< 1 \mu\text{mol N L}^{-1} \text{d}^{-1}$). Still the biomass and the rate of increase with increasing L_N were different in the three communities, but of the same magnitude in BAL and NOR. Third, the fate of the GPP in the communities was generally the same, and the pattern of metabolic flows of assimilated carbon in autotrophic and heterotrophic organisms was comparable in all communities.

Our data do provide strong support for a linear response of biomass and uptake in the lower range of nutrient input rates, but not in the higher range, primarily because of few representative data and because of the deviation from linearity. In the scenario that follows, we assume that the response patterns of biomass and gross uptake are linear with L_N and that the quantitative response given by the slope of the biomass (B) versus L_N and gross uptake (U) versus L_N curves are variables (Fig. 11A). These slopes, which quantify biomass accumulation and gross uptake versus L_N , are termed the response slopes γ_B and γ_U , respectively. We suggest that γ will respond systematically to, for example, the rate of water exchange, time scale of the event, variation in

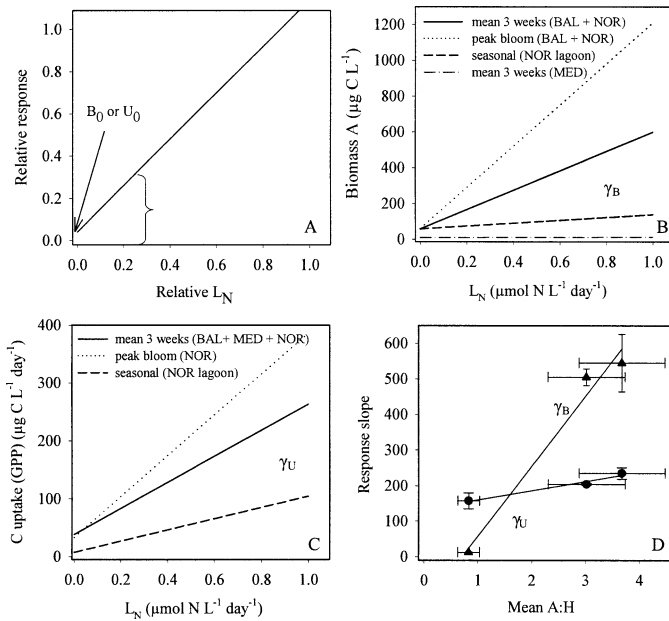


Fig. 11. Conceptual scheme for the response of autotrophic biomass as a function of the nitrogen loading rate (L_N). (A) General scheme of response curve with variable response slope γ and y intercept (y_0) for autotrophic biomass (γ_B and B_0) and GPP (γ_U and U_0); (B) variation of biomass response for different cases (see details in text); (C) variation of GPP response for different cases (see details in text); (D) response slopes for biomass (γ_B) and GPP (γ_U) as a function of the average A:H ratio of the three sampling locations. Bars express 1 standard error; regression coefficients in Table 6.

the grazing pressure, and inherent physiological capabilities of the predominant organisms. The curve intercepts the y axis in B_0 and U_0 for biomass and gross uptake at zero nutrient input, respectively.

We restrict the discussion of the above conceptual model to autotrophic biomass and its gross carbon uptake, or GPP. The concept, however, is in principle applicable also to heterotrophic biomass and GHU. The value of γ_B can in principle vary from zero to the maximum autotrophic community yield times day ($Y_M \times \text{day}$, with Y_M comparable to

Q_0^{-1} ; the inverse subsistence quota for the limiting nutrient [Droop 1983]). The value of γ_U can in principle vary from zero to the maximum growth yield of the autotrophic community (Y_M).

Figure 11B,C illustrates data presented here and some other relevant field data. The upper dotted line of Fig. 11B shows the combined data for BAL and NOR mesocosms and expresses the peak of autotrophic biomass found in these experiments (new data). The solid line expresses the average 3-week response of autotrophic biomass for combined BAL and NOR data, and the lowest nearly horizontal line expresses data for MED (taken from Fig. 6A). The broken line illustrates the response of the average autotrophic biomass during summer (June–September) found in a 5-yr fertilization experiment of an open coastal NOR lagoon system (area 275,000 m², retention time 7–10 d; Olsen et al. unpubl. data). The lagoon was continuously fertilized at rising tides and sampled weekly during June–September in 1998 and 1999 (addition of 0.20 and 0.40 $\mu\text{mol N L}^{-1} \text{d}^{-1}$ in 1998 and 1999, respectively; N:Si:P = 14:2.5:1). The years 1996–1997 and 2000 served as nonfertilized controls. Methods of biomass determination and scientific treatment (e.g., Fig. 1) were identical as in the NOR mesocosm experiments.

The peak biomass response according to the combined BAL and NOR data was typically twice that of their average 3-week response (Table 6). This average response, however, was about 5–6 times higher than the seasonal response in the NOR lagoon, while the 3-week responses of MED was far lower than in the NOR lagoon. The maximum values of biomass found in the lagoon (not shown) were comparable to the average NOR biomass. Factors which may have contributed to these differences include a sustained water exchange of 11–14% per day in the lagoon (e.g., Nixon et al. 1996), a planktonic food web structure better adapted to the final effect of the large grazers, and the grazing capability of the large grazers.

The GPP versus L_N relationship of autotrophs showed smaller variation among experiments than biomass versus L_N (Fig. 11C; Table 6). The 3-week average (solid curve) is for all locations (taken from Fig. 6C). The peak GPP values were taken from NOR (new data) because they are most relevant for comparisons with the lagoon. BAL consistently

Table 6. Regression data with estimates of response slope γ for biomass (γ_B) and for GPP (γ_U) for curves shown in Fig. 11B, C.

Relationship	Case, locations	$\gamma_B \pm 1 \text{ SE}$ $\mu\text{g C } \mu\text{mol N}^{-1} \text{ day}$	$B_0 \pm 1 \text{ SE}$ $\mu\text{g C L}^{-1}$	r^2	p
Biomass					
Sum A versus L_N	Mean 3 week; BAL, NOR	522 ± 40.8	58.2 ± 25.6	0.932	<0.0001
Sum A versus L_N	Mean 3 week; MED	12.0 ± 2.01	9.49 ± 2.65	0.947	<0.05
Sum A versus L_N	Peak bloom; BAL, NOR	1,180 ± 189	91.2 ± 119	0.765	<0.0001
Sum A versus L_N	Seasonal lagoon; NOR	92.5 ± 21.2	13.7 ± 10.1	0.865	<0.05
		$\gamma_U \pm 1 \text{ SE}$ $\mu\text{g C } \mu\text{mol N}^{-1}$	$U_0 \pm 1 \text{ SE}$ $\mu\text{g C L}^{-1} \text{ day}^{-1}$	r^2	p
Gross primary production					
GPP versus L_N	Mean 3 week; BAL, MED, NOR	225 ± 25.7	37.7 ± 15.3	0.836	<0.0001
GPP versus L_N	Peak bloom; NOR	353 ± 12.2	32.9 ± 12.6	0.994	<0.0001
GPP versus L_N	Seasonal lagoon; NOR	97.4 ± 9.63	7.23 ± 4.63	0.981	<0.01

showed higher GPP values (not shown). γ_U for the peak response of GPP was 1.6 times higher than γ_U for the 3-week average response (Table 6), which again was 2–3 times higher than for the seasonal response in the NOR lagoon. The peak GPP values in the lagoon was comparable to the average 3-week values in NOR.

Fig. 11B,C shows a wide variation in autotrophic biomass response to variable nutrient input in coastal locations. Autotrophic biomass and γ_B varied up to ~ 50 and ~ 100 times at equal nutrient input rate, respectively. The variation in GPP response was narrower than that for the biomass (Fig. 11C), even with the higher BAL peak values included (not shown). GPP and γ_U in Fig. 11C varied up to 2.5 and 3.6 times, respectively. Our experiments suggest that grazing can affect γ (Fig. 11D), and both γ_B and γ_U are related to grazing pressure, here expressed as the average A:H ratio for the 3-week periods. γ_B (biomass) appears to respond strongly to this ratio whereas γ_U (GPP) does not. An implication of the results is that only certain taxonomic groups of mesozooplankton, in this case the doliolids belonging to Tunicata (Katechakis et al. 2002), were able to maintain efficient grazing control. A mesozooplankton dominated by copepods cannot maintain the same efficient control. Our mesocosms data represented short-term (3-week) responses, but we believe that they are relevant to open systems.

Again, we emphasize that environmental factors that may cause variation in biomass and GPP are the time scale of the observations, the rate of water exchange, grazing pressure, and high autotrophic lysis rate. Finally, we conclude that the general concept proposed is valid for any time scale and open systems, but we suggest that efforts to quantify the response functions of γ should be made for seasonal to long-term time scales, which are most important for management.

References

- AGAWIN, N. S. R., C. M. DUARTE, AND S. AGUSTÍ. 1998. Growth and abundance of *Synechococcus* sp. in a Mediterranean Bay: Seasonality and relationship with temperature. *Mar. Ecol. Prog. Ser.* **170**: 45–53.
- AGUSTÍ, S., AND C. M. DUARTE. 2000. Strong seasonality in phytoplankton cell lysis in the NW Mediterranean littoral. *Limnol. Oceanogr.* **45**: 940–947.
- BAINES, S. B., AND M. L. PACE. 1991. The production of dissolved organic-matter by phytoplankton and its importance to bacteria—patterns across marine and fresh-water systems. *Limnol. Oceanogr.* **36**: 1078–1090.
- BOOTH, B. C. 1993. Estimating cell concentrations and biomass of autotrophic plankton using microscopy, p. 199–205. *In* P. F. Kemp, B. F. Sherr, E. B. Sherr, and J. J. Cole [eds.], *Handbook of methods in aquatic microbial ecology*. Lewis.
- BØRSHEIM, K. Y., AND G. BRATBAK. 1987. Cell volume to cell carbon conversion factors for a bacterivorous *Monas* sp. enriched from seawater. *Mar. Ecol. Prog. Ser.* **36**: 171–175.
- BORUM, J. 1996. Shallow waters and land/sea boundaries, p. 179–203. *In* B. B. Jørgensen and K. Richardson [eds.], *Eutrophication in coastal marine ecosystems*. American Geophysical Union.
- CLOERN, J. E. 2001. Our evolving conceptual model of the coastal eutrophication problem. *Mar. Ecol. Prog. Ser.* **210**: 223–253.
- COLLIN, F., K. J. HESSE, N. LADWIG, AND U. TILLMANN. 2002. Effects of the large-scale uncontrolled fertilization process along the continental coastal North Sea. *Hydrobiologia* **484**: 133–148.
- CUSHING, D. H., G. F. HUMPHREY, K. BANSE, AND T. LAEVATSU. 1958. Report of the committee on terms and equivalents. *Rapp. Proc. V. ICES* **144**: 15–16.
- DEL GIORGIO, P. A., J. J. COLE, AND A. CIMBLERIS. 1997. Respiration rates in bacteria exceed plankton production in unproductive aquatic systems. *Nature* **385**: 148–151.
- DROOP, M. R. 1983. 25 years of algal growth-kinetics—a personal view. *Bot. Mar.* **26**(3): 99–112.
- DUARTE C. M., AND S. AGUSTÍ. 1998. The CO₂ balance of unproductive aquatic ecosystems. *Science* **281**: 234–236.
- , ———, AND N. S. R. AGAWIN. 2000. Response of a Mediterranean phytoplankton community to increased nutrient inputs: A mesocosm experiment. *Mar. Ecol. Prog. Ser.* **195**: 61–70.
- FAGERBAKKE, K. M., M. HELDAL, AND S. NØRLAND. 1996. Content of carbon, nitrogen, oxygen, sulfur and phosphorus in native aquatic and cultured bacteria. *Aquat. Microb. Ecol.* **10**: 15–27.
- FUHRMAN, J. 1999. Marine viruses and their biogeochemical and ecological effects. *Nature* **399**: 541–548.
- GISMERVIK, I., AND T. ANDERSEN. 1997. Prey switching by *Acartia clausi*: Experimental evidence and implications of intraguild predation assessed by a model. *Mar. Ecol. Prog. Ser.* **157**: 247–259.
- , Y. OLSEN, AND O. VADSTEIN. 2002. Micro- and mesozooplankton response to enhanced nutrient input—a mesocosm study. *Hydrobiologia* **484**: 75–87.
- KATECHAKIS A., H. STIBOR, U. SOMMER, AND T. HANSEN. 2002. Changes in the phytoplankton community and microbial food web of Blanes Bay (Catalan Sea, NW Mediterranean) under prolonged grazing pressure by doliolids (Tunicata), cladocerans or copepods (Crustacea). *Mar. Ecol. Prog. Ser.* **234**: 55–69.
- LIGNELL, R. 1990. Excretion of organic carbon by phytoplankton: Its relation to algal biomass, primary productivity and bacterial secondary productivity in the Baltic Sea. *Mar. Ecol. Prog. Ser.* **68**: 85–99.
- MOUTIN T., T. F. THINGSTAD, F. VAN WAMBEKE, D. MARIE, G. SLAWYK, P. RAIMBAULT, AND H. CLAUSTRE. 2002. Does competition for nanomolar phosphate supply explain the predominance of the cyanobacterium *Synechococcus*? *Limnol. Oceanogr.* **47**: 1562–1567.
- MULLIN, M. M. 1969. Production of zooplankton in the ocean: The present status and problems. *Oceanogr. Mar. Biol. Annu. Rev.* **7**: 293–314.
- NAGATA, T. 2000. Production mechanisms of dissolved organic matter, p. 121–152. *In* D. L. Kirchman [ed.], *Microbial ecology of the ocean*. Wiley-Liss.
- NEJSTGAARD, J. C., B. H. HYGUM, L. J. NAUSTVOLL, AND U. BÅMSTEDT. 2001. Zooplankton growth, diet and reproductive success compared in simultaneous diatom- and flagellate-microzooplankton-dominated plankton blooms. *Mar. Ecol. Prog. Ser.* **221**: 77–91.
- NIXON, S. W., AND M. E. Q. PILSON. 1983. Nitrogen in estuarine and coastal marine ecosystems, p. 565–648. *In* E. J. Carpenter, and D. G. Capone [eds.], *Nitrogen in the marine environment*. Academic.
- , AND OTHERS. 1996. The fate of nitrogen and phosphorous at the land–sea margin of the North Atlantic Ocean. *Biogeochemistry* **35**: 141–180.
- NØRLAND, S. 1993. The relationship between biomass and volume of bacteria, p. 303–306. *In* P. F. Kemp, J. J. Cole, B. F. Sherr, and E. B. Sherr [eds.], *Handbook of methods in aquatic microbial ecology*. Lewis.
- PORTER, K. G., AND Y. S. FEIG. 1980. The use of DAPI for iden-

- tification and enumeration of bacteria and blue-green algae. *Limnol. Oceanogr.* **25**: 943–948.
- PUTT, M., AND D. K. STOECKER. 1989. An experimentally determined carbon: volume ratio for marine “oligotrichous” ciliates from estuarine and coastal waters. *Limnol. Oceanogr.* **34**: 1097–1103.
- SCHIEWER, U. 1998. 30 years’ eutrophication in shallow brackish waters—lessons to be learned. *Hydrobiologia* **363**: 73–79.
- SHURIN, J. B., AND OTHERS. 2002. A cross-ecosystem comparison of the strength of trophic cascades. *Ecol. Letters* **5**: 785–791.
- SOMMER U., AND H. STIBOR. 2002. Copepoda–Cladocera–Tunicata: The role of three major mesozooplankton groups in pelagic food webs. *Ecol. Res.* **17**: 161–174.
- STIBOR, H., AND OTHERS. 2004. Copepods act as a switch between alternative trophic cascades in marine pelagic food webs. *Ecol. Lett.* **7**: 321–328.
- STRAILE, D. 1997. Gross growth efficiencies of protozoan and metazoan zooplankton and their dependence on food concentration, predator–prey weight ratio, and taxonomic group. *Limnol. Oceanogr.* **42**: 1375–1385.
- STRATHMANN, R. R. 1967. Estimating the organic carbon content of phytoplankton from cell volume or plasma volume. *Limnol. Oceanogr.* **12**: 411–418.
- VADSTEIN, O., AND Y. OLSEN. 1989. Chemical composition and PO₄ uptake of limnetic bacterial communities cultured in chemostat under P limitation. *Limnol. Oceanogr.* **34**: 939–946.
- , H. STIBOR, B. LIPPERT, K. LØSETH, W. ROEDERER, L. SUNDT-HANSEN, AND Y. OLSEN. 2004. Moderate increase in the biomass of omnivorous copepods may ease grazing control of planktonic algae. *Mar. Ecol. Prog. Ser.* **270**: 199–207.
- VERITY, P. G., AND C. LANGDON. 1984. Relationships between lorica volume, carbon, nitrogen, and ATP content of tintinnids in Narragansett Bay. *J. Plankton Res.* **6**: 859–868.
- VÉZINA, A. F., AND T. PLATT. 1988. Food web dynamics in the ocean. I. Best-estimates of flow networks using inverse methods. *Mar. Ecol. Prog. Ser.* **42**: 269–287.
- WATERBURY, J. B., S. W. WATSON, F. W. VALOIS, AND D. G. FRANKS. 1986. Biological and ecological characterisation of the marine unicellular cyanobacterium *Synechococcus*, p. 71–120. *In* T. Platt and W. K. W. Li [eds.], *Photosynthetic picoplankton*. Can. Bull. Fish. Aquat. Sci. **214**.
- WILLIAMS, P. J. LEB. 1995. Evidence for the seasonal accumulation of carbon-rich dissolved organic material, its scale in comparison with changes in particulate material and the consequential effect on net C/N assimilation ratios. *Mar. Chem.* **51**: 17–29.
- VOLLENWEIDER, R. A. 1976. Advances in defining critical load levels for phosphorus in lake eutrophication. *Mem. Ist. Ital. Idrobiol.* **33**: 53–83.
- ZEHR, J. P., AND OTHERS. 2001. Unicellular cyanobacteria fix N-2 in the subtropical North Pacific Ocean. *Nature* **412**: 635–638.

Received: 7 January 2005

Accepted: 25 April 2005

Amended: 16 May 2005